DE GRUYTER OPEN

Archives of Hydro-Engineering and Environmental Mechanics
Vol. 61 (2014), No. 1–2, pp. 39–60
DOI: 10.1515/heem-2015-0003

Modeling of Water Flows around a Circular Cylinder with the SPH Method

Kazimierz Szmidt, Benedykt Hedzielski

Institute of Hydro-Engineering, Polish Academy of Sciences, ul. Kościerska 7, 80-328 Gdańsk, Poland,
e-mail: jks@ibwpan.gda.pl

(Received May 21, 2014; revised November 05, 2014)

Abstract

The paper describes the SPH modeling of a plane problem of fluid flow around a rigid circular cylinder. In the model considered, the cylinder is placed in a rectangular fluid domain at a certain distance from a horizontal plane boundary, and it is subjected to fluid flow forces. The fluid motion is induced by a piston type generator. The generator – fluid system starts to move from rest at a certain moment of time. The work aims at a discrete description of the fluid flow around the cylinder and, at the same time, calculation of the pressure distribution along the circumference of the cylinder and the resultant of the pressure on the cylinder. In order to solve the initial value problem considered, a new SPH formulation of boundary conditions on the cylinder surface is proposed which match the physical condition for the fluid velocity at this boundary. For a viscous fluid, an approximate description of the stress tensor is formulated which allows to reduce the differentiation of field functions to the first order in calculating the shear forces in the SPH approach.

Key words: transient water wave, SPH modeling, boundary conditions, approximation of shear forces

1. Introduction

Wave induced flows around a cylinder and associated hydrodynamic forces on it have been of special interest in offshore engineering and, at the same time, in theoretical hydrodynamics. The general problem of the flows for viscous fluids seems to be constantly in question, because of the complicated flow regimes, which depend on the ambient velocity distribution, turbulence and the presence of a free surface. On the other hand, in analysis of the water waves, the fluid viscosity is important only in a very small vicinity of the fluid boundary (within boundary layers of very small thickness) and therefore, in description of the waves, it is justified to neglect to fluid viscosity. As concerns the waves, serious difficulties emerge in theoretical description of finite (big) displacements of fluid particles and in cases of the fluid fragmentation. Therefore, in analysis of such problems we usually resort to simplified models of description of the phenomenon. In these descriptions, we frequently resort to discrete

methods in which continuum is substituted by a number of nodal points. Field variables of a problem such as pressure, density and momentum are represented by point variables associated with chosen points. With respect to the problem considered, the Smooth Particle Hydrodynamics (SPH) formulation seems to be of practical interest, since it serves equally well for continuous and discontinuous media. The SPH is a purely Lagrangian mesh free method in which the motion of the fluid is simulated by a motion of a number of material particles. The method aims at computing distribution of these particles and associated field variables at chosen moments of time. The literature on the subject is considerable. In the last two decades a number of papers has appeared where particular numerical solvers of the method have been developed and successfully applied to various problems of hydrodynamics. Fundamentals of the SPH method are presented in the important works of Monaghan (1992, 2005). A detailed discussion on the SPH application to various problems of hydrodynamics may be found in Liu and Liu monograph (2006) which also contains a vast bibliography on the subject. The SPH formulation has been successfully applied in analysis of the interfacial flows (Colagrossi and Landrini 2003), in simulation of near-shore solitary mechanics (Lo and Shao 2002) and in analysis of the dam break problem (Bonet and Lok 1999, Staroszczyk 2010, Grenier et al 2009) and in the description of multi-phase flows (Hu and Adams 2006). As concerns the flow around a circular cylinder, Morris et al (1997) considered a periodic flow past a cylinder for very low Reynolds numbers. The SPH simulation was run for material particles placed on a hexagonal lattice with a very dense spacing equal to 0.002 m. The solutions obtained were compared with results of the finite element method. A good agreement was obtained for bulk of the flow, although small discrepancies emerge in the SPH description of velocities near the cylinder. A similar problem of the flow past a periodic lattice of cylinders was investigated by Ma and Ge (2008). These authors investigated the SPH solutions for different values of smoothing length h and isothermal sound speeds. For the length h smaller than $1.2d$, where d denotes spacing of the material particles, some deviations of results were observed for a set of formulations considered.

With respect to the non-linear water waves, considered in this paper, the advantage of the SPH approach over another discrete methods of descriptions is that this method serves equally well for small and finite displacements of fluid particles from their initial positions. The method suffers from its relative weakness in describing boundary conditions, especially at the fluid – solid boundary, and problems, where field variables depend on higher order space derivatives of the velocity field. Therefore, in application of the method to analysis of flows around the cylinder, a special care must be taken in formulating boundary conditions at the fluid – cylinder interface. At the same time, in describing dissipative forces for viscous fluids, it is desirable to construct a consistent approximation of viscous terms entering momentum equations. In order to answer the question about usefulness of the method in description of the fluid flows around a cylinder, some particularly simple examples, of the initial-value problems considered, are presented in this paper. The main attention of this research

is paid on formulations of the boundary conditions and approximations in the description of shear forces.

2. Governing Equations of Hydrodynamics

In order to keep the further discussion clear, we attach here some fundamental equations of theoretical hydrodynamics. The principle of mass conservation of moving fluid leads to the equation of continuity

$$\frac{d\rho}{dt} + \rho \operatorname{div} \boldsymbol{v} = \frac{\partial \rho}{\partial t} + \operatorname{div}(\rho \boldsymbol{v}) = 0. \tag{1}$$

For the viscous compressible fluid, the equations of motion are

$$\rho \frac{du^i}{dt} = \rho b^i + \frac{\partial T^{ij}}{\partial x_j}, \tag{2}$$

where b^i denotes the body force, and T^{ij} is the stress tensor, dependent on the rate of the deformation tensor

$$D^{ij} = \frac{1}{2}\left(\frac{\partial u^i}{\partial x_j} + \frac{\partial u^j}{\partial x_i}\right). \tag{3}$$

For isotropic incompressible fluids, the stress tensor may be written in the following form

$$T^{ij} = -p\delta^{ij} + 2\mu D^{ij}, \tag{4}$$

where p denotes the fluid pressure, δ^{ij} is the Kronecker delta and μ is the dynamic viscosity coefficient.

For the incompressible fluids, the momentum equations read

$$\rho \frac{du^i}{dt} = -\frac{\partial p}{\partial x_i} + \rho b^i + \mu \nabla^2 u^i. \tag{5}$$

With respect to the SPH formulation, the pressure – density relation for the fluid is usually adopted in the following form (Monaghan 1992)

$$p(\rho) = P_0 \left[\left(\frac{\rho}{\rho_0}\right)^{\gamma} - 1\right]. \tag{6}$$

In this equation, P_0 and ρ_0 denote the reference pressure and density, and the parameter γ is usually taken as 7 for water and 1.4 for air (Colagrossi and Landrini 2003). The corresponding sound speed c_s is given by

$$c_s = \sqrt{\frac{\gamma P_0}{\rho_0}}. \tag{7}$$

The employment of the equation of state (6) simplifies calculation of the pressure for a problem considered, which is usually reduced to the unknown velocity components and the fluid density.

3. The SPH Formulation

The SPH is an interpolation method based on the concept of integral representation of a function, say $f(\boldsymbol{r})$, by the following integral

$$< f(\boldsymbol{r}) >= \int_S f(\boldsymbol{r}')W\left(\left|\boldsymbol{r}-\boldsymbol{r}', h\right|\right) dS', \tag{8}$$

where S is the domain of integration, and $W(|\boldsymbol{r}-\boldsymbol{r}'|, h)$ is the so called smoothing function, or smoothing kernel function, or interpolating kernel, or simply kernel in the SPH literature. The parameter h in this equation is the smoothing length responsible for a shape of the kernel. The left hand side of equation (8) is called the interpolant of $f(\boldsymbol{r})$ (Monaghan 1992), since it is only a certain approximation of the original function. With respect to this approximation, in what follows, we omit the brackets on the left hand side of the integral formula. In the case the kernel is the Dirac delta function $\delta(\boldsymbol{r}-\boldsymbol{r}')$, the equation defines the well known identity $f(\boldsymbol{r}) = \int_S f(\boldsymbol{r}')\delta(\boldsymbol{r}-\boldsymbol{r}')dS'$. The kernel $W(\boldsymbol{r}-\boldsymbol{r}', h)$ in equation (8) is usually chosen to be an even function, which should satisfy a number of conditions. The first of them is the unity condition

$$\int_S W(\boldsymbol{r}-\boldsymbol{r}', h)dS' = 1. \tag{9}$$

The second one is the delta function property

$$\lim_{h\to 0} W(\boldsymbol{r}-\boldsymbol{r}', h) = \delta(\boldsymbol{r}-\boldsymbol{r}'). \tag{10}$$

For practical reasons, the kernel should also satisfy the compact condition

$$W(\boldsymbol{r}-\boldsymbol{r}', h) = 0 \quad \text{when} \quad \left|\boldsymbol{r}-\boldsymbol{r}'\right| > R, \tag{11}$$

where R is the radius of a circular support domain centred at $\boldsymbol{r}$ for a two dimensional case, or a spherical support domain in a three dimensional case.

In addition to the above conditions, the kernel is assumed to be the non-negative function within the support domain. It is also desired this function should monotonically decrease with the increasing distance away from the field point $\boldsymbol{r}$. Finally, the kernel function should be continuous and sufficiently smooth to ensure accurate approximation of a function and its space derivatives.

In literature on the subject there exist various forms of the kernel functions with certain restrictions imposed on them to ensure desired properties, listed above. Frequently used are spline functions of a chosen order; for example: quadratic, cubic or quartic spline functions. Among others, a Gaussian function is of primary importance. For the two-dimensional case, considered in this paper, the Gaussian kernel reads

$$W(r, h) = \frac{1}{\pi h^2}\exp\left(-q^2\right), \quad \text{where} \quad q = \frac{r}{h}, \quad r^2 = x^2 + y^2. \tag{12}$$

According to Monaghan (1992), it is always best to assume the kernel is a Gaussian, and thus, in the further part of this work we will only consider the Gaussian kernels. In general, at points of the boundary of a finite support domain, the Gaussian kernel function is different from zero and, at the same time, the integral of the kernel over the support domain does not equal to unity. Therefore, in order to overcome this inconsistency, it is reasonable to take into account the normalized kernel (Colagrossi, Landrini 2003)

$$W_N = \frac{\frac{1}{\pi h^2}\left[\exp\left(-q^2\right) - \exp\left(-R^2\right)\right]}{\frac{1}{\pi h^2}\int\limits_S \left[\exp\left(-q^2\right) - \exp\left(-R^2\right)\right] dS'} = \\ = \frac{\left[\exp\left(-q^2\right) - \exp\left(-R^2\right)\right]}{\int\limits_S \left[\exp\left(-q^2\right) - \exp\left(-R^2\right)\right] dS'}, \quad R = \frac{\delta}{h}. \tag{13}$$

One can check that this equation satisfies the unity condition (9).

In the SPH formulation, the continuum is replaced by a set of material particles and the continuous integral interpolation is approximated by a discrete summation interpolation. In the discrete approach, the infinitesimal volume (surface) dS' in the integrand (8) is replaced by the finite volume V_b of a particle b. Thus, the elementary volume V_b, the density ρ_b and the mass m_b of this particle are related by

$$m_b = \rho_b V_b. \tag{14}$$

With respect to this formula, the continuous SPH representation for $f(\boldsymbol{r})$ is substituted by the discrete particle approximation expressed in the following form

$$f(r) = f(\boldsymbol{r})|_a = f_a = \sum_{b=1}^{N} \frac{m_b}{\rho_b} f(\boldsymbol{r}_b)\ W(\boldsymbol{r} - \boldsymbol{r}_b, h), \tag{15}$$

where b denotes the particle label and the summation is taken over all particles in the finite support domain of a point (particle) $\boldsymbol{r}_a$.

For example, the above interpolation formula gives the following estimate for the density at the point $\boldsymbol{r} = \boldsymbol{r}_a$

$$\rho_a = \sum_b \frac{m_b}{\rho_b} \rho_b W_{ab} = \sum_b m_b W_{ab}. \tag{16}$$

With respect to the discrete formulation considered, the unity condition of the kernel function is preserved by the transformation of the kernel W_{ab} into another form, known as the Shepard function (Shepard kernel), defined by

$$W_{ab}^S = \frac{W_{ab}}{\sum\limits_{b=1}^{N} V_b W_{ab}}. \tag{17}$$

The essential feature of the discrete interpolant is that it enables us to construct a differentiable approximation of a function from its values at particle nodal points by means of the differentiable kernel. In the discrete approximation of fundamental equations of fluid dynamics one needs to construct approximations of the gradient and divergence differential operators. Following the interpolation, mentioned above, such operators may be obtained by a direct differentiation of the kernel function. A more detailed discussion on differential operators with desired properties may be found in papers by Monaghan (1992, 2005). To make the further discussion clear, we attach here interpolations of the gradient and divergence operators given in that papers. The interpolation of the gradient of a scalar function f at particle a reads

$$\nabla f_a = \rho_a \sum_b m_b \left(\frac{f_a}{\rho_a^2} + \frac{f_b}{\rho_b^2} \right) \nabla_a W_{ab} \tag{18}$$

and, the divergence of a vector field, say velocity field $\boldsymbol{v}$ at particle a, can be found from

$$(\nabla \cdot \boldsymbol{v})_a = \frac{1}{\rho_a} \sum_b m_b (\boldsymbol{v}_b - \boldsymbol{v}_a) \cdot \nabla_a W_{ab}. \tag{19}$$

It should be stressed that in the SPH approach we have no unique formulation of equations describing field variables. For instance, the divergence of the velocity field described by equation (19) may be also written in a simple way as

$$\operatorname{div}(\boldsymbol{v}_a) = (\nabla \cdot \boldsymbol{v})_a = \frac{1}{\rho_a} \sum_b m_b \boldsymbol{v}_b \cdot \nabla_a W_{ab}, \tag{20}$$

or in the symmetrical form

$$\operatorname{div}(\boldsymbol{v}_a) = (\nabla \cdot \boldsymbol{v})_a = \rho_a \sum_b m_b \left[\frac{\boldsymbol{v}_a}{\rho_a^2} + \frac{\boldsymbol{v}_b}{\rho_b^2} \right] \cdot \nabla_a W_{ab}. \tag{21}$$

At the same time, for a Gauss kernel of the form

$$W^{\bullet} = \frac{1}{K_2} \exp\left[-\left(\frac{r}{h} \right)^2 \right], \tag{22}$$

where K_2 corresponds to the denominator in equation (13), simple manipulations give

$$\nabla_a W_{ab} = \frac{2}{h^2} (\boldsymbol{r}_b - \boldsymbol{r}_a) W_{ab}^{\bullet}. \tag{23}$$

From substitution of this result into equation (19) it follows

$$\rho_a (\nabla \cdot \boldsymbol{v})_a = \frac{2}{h^2} \sum_b m_b (\boldsymbol{v}_a - \boldsymbol{v}_b) \cdot (\boldsymbol{r}_a - \boldsymbol{r}_b) \, W_{ab}^{\bullet}. \tag{24}$$

This equation shows, that the contribution from particle b to the divergence of the velocity at particle a is described by the symmetric formula

$$2m_b(\boldsymbol{v}_a - \boldsymbol{v}_b) \cdot (\boldsymbol{r}_a - \boldsymbol{r}_b) \frac{W^{\bullet}_{ab}}{h^2}. \tag{25}$$

It may be seen that this contribution is positive if the particles are moving away from each other, as it should be. The vorticity at the particle a is obtained in a similar way by

$$\rho_a(\nabla \times \boldsymbol{v})_a = \frac{1}{\rho_a} \sum_b m_b(\boldsymbol{v}_b - \boldsymbol{v}_a) \times \nabla_a W_{ab}. \tag{26}$$

By virtue of the equation of continuity, the density evolution is described by the following interpolation formula (Monaghan 1992)

$$\left.\frac{d\rho}{dt}\right|_a = \sum_b m_b(\boldsymbol{v}_a - \boldsymbol{v}_b)\nabla_a W_{ab}. \tag{27}$$

For a non-viscous, slightly compressible fluid, the interpolation of the momentum equations gives

$$\begin{aligned} \frac{d\boldsymbol{v}_a}{dt} &= -\sum_b m_b \left(\frac{P_a}{\rho_a^2} + \frac{P_b}{\rho_b^2}\right) \frac{\partial}{\partial x}(W_{ab}) \,, \\ \frac{d\boldsymbol{v}_a}{dt} &= -\sum_b m_b \left(\frac{P_a}{\rho_a^2} + \frac{P_b}{\rho_b^2}\right) \frac{\partial}{\partial y}(W_{ab}) - g \,, \end{aligned} \tag{28}$$

where $\boldsymbol{v}_a = (u_a, v_a)$ and g is the gravitational acceleration.

Substituting equation (19) into the last relations one obtains

$$m_a \frac{d\boldsymbol{v}_a}{dt} = \sum_b 2\frac{m_a m_b}{h^2} \left[\frac{p_a}{\rho_a^2} + \frac{p_b}{\rho_b^2}\right] (\boldsymbol{r}_a - \boldsymbol{r}_b) W_{ab} - m_a \boldsymbol{g}, \tag{29}$$

where $\boldsymbol{g} = (0, g)$.
From the last equation it follows that the force on the particle a from the particle b is

$$\boldsymbol{F}_{ab} = 2\frac{m_a m_b}{h^2} \left[\frac{p_a}{\rho_a^2} + \frac{p_b}{\rho_b^2}\right] (\boldsymbol{r}_a - \boldsymbol{r}_b)\, W_{ab}, \tag{30}$$

which shows that the pressure gradient in the SPH formulation produces a symmetric central force between pairs of particles.

4. Boundary Conditions

In applications of the SPH method to water wave mechanics, the problem of a particle formulation of boundary conditions at the fluid boundary emerges. Since the method

applies for collection of material particles moving in space, the fluid boundary is defined as a set of conditions imposed on particles reaching points at this boundary. A relatively simple, is the description of the free surface of the fluid which, in the material description, employed in the SPH approach, is defined by positions of the material particles forming this surface. It should be stressed however, that only particles at, - or near the boundary, contribute to the summation of the particles interactions. With respect to these particles, their finite supports are usually truncated by this boundary, and thus, some discrepancies in calculating the pressure and the fluid density may occur. Even more serious problems are met in formulation of the SPH boundary conditions at solid, fixed or moving, boundaries of the fluid domain. For a solid (rigid), free-slip boundary, the normal component of the velocity field should be equal to zero. An example of such a boundary is the case of a straight line solid boundary, usually met in analysis of gravitational waves propagating in water of finite depth, as illustrated in Fig. 1.

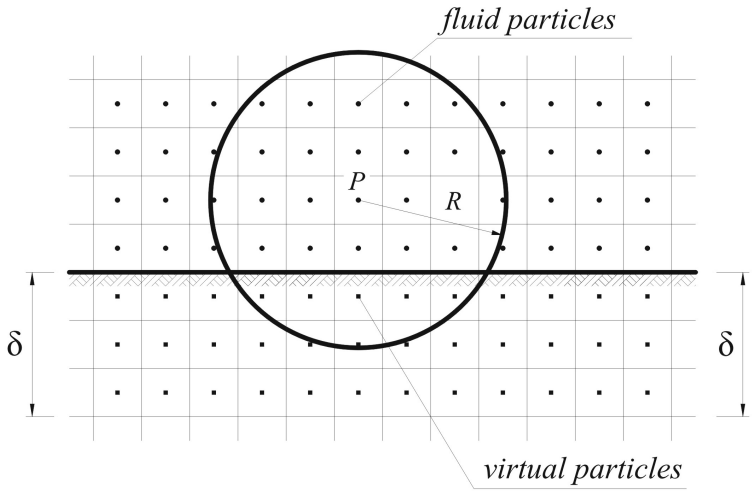

Fig. 1. Straight line boundary and virtual particles. The support domain of particle P is defined by a circle of radius R

In order to solve boundary condition at this boundary, additional, virtual (ghost) particles are placed outside the fluid domain, as it is marked in this figure. Such a model of solution of the boundary condition with additional mirror particles has been used by Lo and Shao (2002) in simulating near-shore solitary wave mechanics and by Staroszczyk (2010) in simulating water flow, generated by a dam break. Since in the SPH approach we deal with finite support domains, the additional particles are distributed within a strip of finite width δ, which equals to the assumed radius of a typical support domain within the fluid. The additional particles have the same mass, density and velocity as their counterparts in the fluid domain, with obvious restriction that normal components of the velocity have equal values and opposite signs. For

a viscous fluid also the tangent components of the velocity field within the fluid and at virtual particles have opposite signs. In the case shown in Fig. 1, the use of the mirror particles corresponds directly to solution of a symmetrical problem in continuum where the bottom line is the symmetry line of a problem domain considered. A remark is needed. The SPH equations are usually written for particles inside the fluid domain. Therefore, for the inner particles placed near the boundary, the contribution of virtual particles in the interpolation over the support domain is necessarily less than that of the inner particles (the contribution is the same only for particles at the boundary). It means that in the SPH model, a phenomenon of attraction of the fluid particles by solid boundaries may occur. Such an attraction is induced by forces, resulting from non-equal contributions of pressure gradients, which act on material particles near the boundary. In the literature on the subject several attempts have been made to prevent the inner fluid particles from accumulating in the vicinity of solid boundaries. Usually, additional boundary particles are employed to generate repulsive forces on fluid particles (Morris et al 1997, Monaghan 2005, Ataie-Ashtiani et al 2008, Monaghan and Kajtar 2009). These repulsive forces prevent the real particles from penetration of the boundary. A way to specify the forces is to use a Lenard-Jones force acting between the centers of the particles (Monaghan 2005). On the other hand, such forces, acting on particles moving parallel to the boundary may cause large disturbances to flow near the boundary. In fact, such repulsive forces do not result from a solution in fluid dynamics, and therefore their employment should be made with a great care. The problem becomes more complicated in the case of a boundary formed by a set of segments intersecting at corner points or in the case of a curved boundary. If the segments intersect at right angles, the best solution is to use mirror reflection of material particles within a strip along the boundary. In the case of an arbitrary angle of intersection, or in the case of curved boundary however, it is not possible to find a unique distribution of virtual (additional) particles to solve the boundary conditions. As far as curved boundaries are concerned, a special boundary treatment is described in Liu and Liu (2009), where except real particles within a circular fluid domain, virtual boundary (type I) and, - exterior (type II) particles are used to solve the boundary conditions at the domain circumference. Despite of several attempts mentioned above, the problem of a proper formulation of boundary conditions in the SPH method is still an open question.

In the following, an approximate solution of boundary conditions at curved boundary is presented, which may be also used for boundaries formed by intersecting straight segments. For a curved fluid – solid boundary, shown schematically in Fig. 2, it is not possible to employ the above mentioned approach directly, and therefore another method of solution is proposed. Like in the above mentioned case, the normal components of the velocity field should be equal to zero at this boundary. In order to solve this boundary condition in the SPH approach, let us consider the case of non-viscous fluid and a set of artificial particles placed at this boundary or near the boundary on the solid side. The spacing of these particles is assumed to be equal to

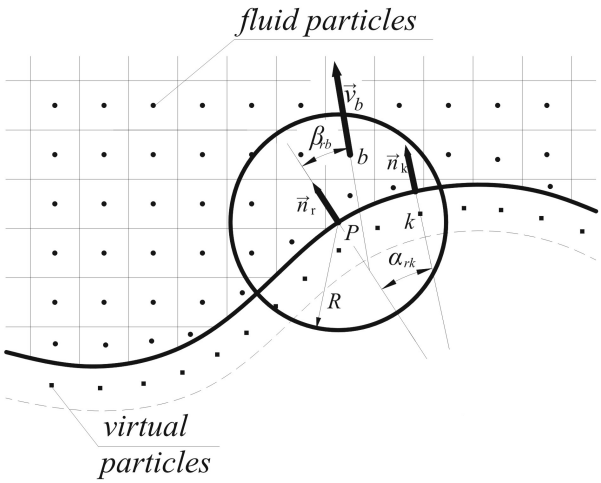

Fig. 2. Curved boundary and additional particles. The support domain of particle P is defined by a circle of radius R

the spacing of the fluid particles at the initial moment of time. The positions of the boundary particles are fixed in space and time. For a given instant of time, the normal velocity components at the boundary points, following the fluid particles in the SPH method, are in a general case different from zeros. These additional artificial boundary particles are assumed to have such normal velocities, unknown at this moment, that the final velocity, dependent both on the fluid particles and the additional particles, are equal to zeros at these boundary points. Since the interpolation in the SPH method is a linear operation, one can divide the particle contribution to the velocity field into two parts, each of which corresponds either to the fluid or – to the boundary particles. With respect to the description in Fig. 2, it is sufficient to assume that all velocities of these artificial particles are normal to the boundary. A normal velocity component at the space point r of the boundary is expressed in the following form

$$v_r = \sum_{b}^{\text{fluid}} \frac{m_b}{\rho_b} v_b^f \cos\beta_{rb} W_{rb} + \sum_{k}^{\text{virtual}} V_k v_k^n \cos\alpha_{rk} W_{rk}, \tag{31}$$

where v_b^f is the velocity of a fluid particle placed in support domain, β_{rb} is the angle between the fluid velocity and the normal direction to the boundary at the space point r, $V_k = V = \text{const.}$ is an elementary volume associated with the virtual particles v_k^n is the unknown, normal velocity of virtual particle and α_{rk} is the angle between the normal directions to the boundary at the space points r and k, respectively.

The second part of the right hand side of this equation denotes the contribution of the unknown normal components of the virtual particles. Equations (31) are written for all points of the boundary. The system of equations obtained in this way enables us to calculate the normal components of the velocity of the virtual particles. In the case

of a viscous fluid, both the normal and tangent components of the velocity field at the boundary points should be equal to zero. In this case, two sets of equations of the form (31) are written for the boundary points, each of which corresponds to chosen components of the velocity vectors at these points. It should be stressed however, that the accuracy of the formulation depends on the number of particles within the support domain for each point of the boundary and therefore, one must expect a relative discrepancy in the solution accuracy in the vicinity of corner points. The solution to the boundary conditions presented above leads to a certain extension of computation time and thus it may be cumbersome to apply it, especially for complicated geometry of the boundary. Meanwhile, the proposal described by equation (31) has been used in solution to the boundary conditions at the cylinder surface in illustration examples presented in the further section of this paper.

5. Viscous Fluids – SPH Treatment of Shear Forces

In equation (2), describing the viscous fluid motion, the term with the stress tensor is substituted with the following one

$$\frac{1}{\rho}\frac{\partial T^{ij}}{\partial x^j} = \frac{\partial}{\partial x^j}\left(\frac{T^{ij}}{\rho}\right) + \frac{T^{ij}}{\rho^2}\frac{\partial \rho}{\partial x^j}. \tag{32}$$

From substitution of this relation into equation (2) one obtains

$$\frac{dv^i}{dt} = b^i + \sum_b m_b \left[\frac{T_a^{ij}}{\rho_a^2} + \frac{T_b^{ij}}{\rho_b^2}\right]\frac{\partial}{\partial x^j}(W_{ab}). \tag{33}$$

The formula is similar to equations (28), written for non-viscous fluids.

The stress tensor components, entering equations (33), depend on the rate of deformation tensor as it is described by equation (4). With respect to the SPH formulation, the components of the momentum equations are

$$\begin{aligned}
\frac{du_a}{dt} &= -\sum_b m_b \left(\frac{P_a}{\rho_a^2} + \frac{P_b}{\rho_b^2}\right)\frac{\partial}{\partial x}(W_{ab}) + \\
&+ \sum_b m_b \left(\frac{\mu_a D_{1j}^a}{\rho_a^2} + \frac{\mu_b D_{1j}^b}{\rho_b^2}\right)\frac{\partial}{\partial x_a^j}(W_{ab}), \\
\frac{dv_a}{dt} &= -\sum_b m_b \left(\frac{P_a}{\rho_a^2} + \frac{P_b}{\rho_b^2}\right)\frac{\partial}{\partial y}(W_{ab}) + \\
&+ \sum_b m_b \left(\frac{\mu_a D_{2j}^a}{\rho_a^2} + \frac{\mu_b D_{2j}^b}{\rho_b^2}\right)\frac{\partial}{\partial x_a^j}(W_{ab}) - g.
\end{aligned} \tag{34}$$

Equations (34) suggest, that in order to calculate the velocity of material points in the problem domain, it is necessary to perform the two steps calculations: – in the

first step the components of the rate of the deformation tensor should be obtained and then – in the second step, the shear tensor components should be defined. With such a procedure however it is not possible to obtain proper results in the areas of fluid close to the fluid boundary.

On the other hand, a direct calculation of the second order space derivatives of the velocity field, entering equation (5), leads to interpolation with the second order derivative of the kernel function. The letter approach however does not fulfil the so called reproducing conditions, and thus, such a method of solution is not admissible.

Therefore, with respect to these difficulties for viscous fluids, it is reasonable to resort to approximate description of the stress tensor by a direct calculation of its components by means of mechanics of individual material particles carrying the mass and momentum and interacting with each other. Thus, let us consider two material particles shown schematically in Fig. 3.

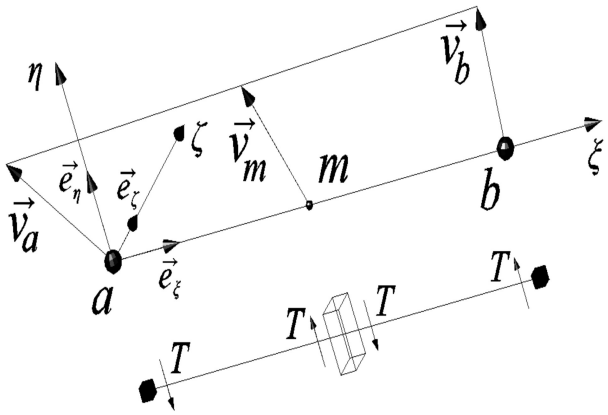

Fig. 3. Shear forces between two material particles

Interaction forces between these particles are reduced to the central force with direction defined by positions of the particles in space and the second force normal to the first one. The central force is associated with the average pressure and the transverse force – with the shear force between these particles. To simplify the discussion, let us consider the case of incompressible fluid and the corresponding, viscous term of the stress tensor

$$T^{ij} = \mu\left(\frac{\partial v^i}{\partial x^j} + \frac{\partial v^j}{\partial x^i}\right). \tag{35}$$

For the two particles (a, b) in the figure, it is convenient to introduce the unit vector

$$\boldsymbol{e} = \frac{\boldsymbol{r}_{ab}}{|\boldsymbol{r}_{ab}|} = \frac{\boldsymbol{r}_b - \boldsymbol{r}_a}{r} = \frac{1}{r}\left[(x_b - x_a)\,\boldsymbol{i} + (y_b - y_a)\,\boldsymbol{j} + (z_b - z_a)\,\boldsymbol{k}\right]. \tag{36}$$

At the same time,

$$\frac{\partial v^i}{\partial x^j} = \frac{\partial v^i}{\partial r}\frac{\partial r}{\partial x^j} = \frac{\partial v^i}{\partial r}\frac{(x_b - x_a)^j}{r} \cong \frac{\Delta v^i}{\Delta r}\frac{(x_b - x_a)^j}{r} \cong \frac{1}{r^2}(v_b - v_a)^j (x_b - x_a)^j . \quad (37)$$

From substitution of (37) into equation (35) one obtains

$$T^{ij} \cong \frac{\mu}{r}\left[e_i V^j_{ab} + e_j V^i_{ab}\right], \quad (38)$$

where

$$V^j_{ab} = (v_b - v_a)^j . \quad (39)$$

The stress tensor is assumed to vary continuously between the points a and b, and therefore, in the midpoint m, the following condition should be satisfied

$$\mu_k \left[e_i (V_{am})^j + e_j (V_{am})^i\right] = \mu_l \left[e_i (V_{mb})^j + e_j (V_{mb})^i\right] , \quad (40)$$

where μ_k and μ_l denote the viscosity coefficients at points a and b, and

$$\begin{aligned} &V_{am} = V_m - V_a, \quad V_{mb} = V_b - V_m, \\ &V_{am} + V_{mb} = V_b - V_a = V_{ab}. \end{aligned} \quad (41)$$

With respect to the midpoint m, the components of the stress tensor becomes

$$\begin{aligned} T^{ij}_{am} &= \frac{\mu_k}{r_{am}}\left[e_i (V_{am})^j + e_j (V_{am})^i\right] , \\ T^{ij}_{mb} &= \frac{\mu_l}{r_{mb}}\left[e_i (V_{mb})^j + e_j (V_{mb})^i\right] . \end{aligned} \quad (42)$$

These components are equal to each other and therefore, from substitution of (41) into the last formulae, the following relations are obtained

$$(V_{am})^j = \frac{\mu_l}{\mu_k + \mu_l}(V_{ab})^j, \quad (V_{am})^i = \frac{\mu_l}{\mu_k + \mu_l}(V_{ab})^i. \quad (43)$$

Knowing that $T^{ij}_{am} = T^{ij}_{mb} = T^{ij}_{ab}$ we arrive at the following result

$$T^{ij}_{ab} = \frac{2}{r}\frac{\mu_k \mu_l}{\mu_k + \mu_l}\left[e_i (V_{ab})^j + e_j (V_{ab})^i\right]. \quad (44)$$

For the case $\mu_k = \mu_l = \mu$ the equation simplifies to the form

$$T^{ij}_{ab} = \frac{\mu}{r}\left[e_i (V_{ab})^j + e_j (V_{ab})^i\right]. \quad (45)$$

The last formulae are similar to descriptions of the inter-particle averaged shear tensors $\boldsymbol{T}^{v}_{ij}$ presented in Hu and Adams (2006), and in Grenier et al (2009).

In accordance with equation (44), for the two-dimensional problem considered, the momentum equations for the incompressible viscous fluid are written in the following form

$$\begin{aligned}
\frac{du}{dt} &= -\sum_b m_b \left(\frac{p_a}{\rho_a^2} + \frac{p_b}{\rho_b^2}\right)\frac{\partial W_{ab}}{\partial x_a} + \\
&+ \sum_b m_b \left[\left(\frac{T_a^{11}}{\rho_a^2} + \frac{T_b^{11}}{\rho_b^2}\right)\frac{\partial W_{ab}}{\partial x_a} + \left(\frac{T_a^{12}}{\rho_a^2} + \frac{T_b^{12}}{\rho_b^2}\right)\frac{\partial W_{ab}}{\partial y_a}\right], \\
\frac{dv}{dt} &= -\sum_b m_b \left(\frac{p_a}{\rho_a^2} + \frac{p_b}{\rho_b^2}\right)\frac{\partial W_{ab}}{\partial y_a} - g + \\
&+ \sum_b m_b \left[\left(\frac{T_a^{21}}{\rho_a^2} + \frac{T_b^{21}}{\rho_b^2}\right)\frac{\partial W_{ab}}{\partial x_a} + \left(\frac{T_a^{22}}{\rho_a^2} + \frac{T_b^{22}}{\rho_b^2}\right)\frac{\partial W_{ab}}{\partial y_a}\right].
\end{aligned} \tag{46}$$

where the components of the shear forces are

$$\begin{aligned}
T_{ab}^{11} &= \frac{2}{r^2}\frac{\mu_a\mu_b}{\mu_a+\mu_b}\left[2(x_b - x_a)(u_b - u_a)\right], \\
T_{ab}^{12} &= \frac{2}{r^2}\frac{\mu_a\mu_b}{\mu_a+\mu_b}\left[(x_b - x_a)(v_b - v_a) + (y_b - y_a)(u_b - u_a)\right], \\
T_{ab}^{22} &= \frac{2}{r^2}\frac{\mu_a\mu_b}{\mu_a+\mu_b}\left[2(y_b - y_a)(v_b - v_a)\right],
\end{aligned} \tag{47}$$

where $T_{ab} = T_a = T_b$ for each pair of individual material particles.

In the discussion on shear forces in viscous fluids presented so far, the shear stress tensor was obtained by means of substitution of exact differentiation of the velocity components, entering the formulae for the rate of the deformation tensor, by quotients of differences of the velocity components at material particles contributed in the interpolation procedure applied. Such a procedure seems to be justified, provided that the distance between a pair of particles is not too big, and, at the same time, the velocity distribution over a support domain of a given particle is sufficiently smooth.

6. Numerical Experiments

In order to illustrate the discussion presented in the preceding sections, in what follows we will consider some numerical experiments for a fluid flow in a plane, rectangular basin of water as it is shown schematically in Fig. 4.

The motion of the incompressible fluid is induced by a piston-type generator placed at the left hand side of the fluid domain. The generator – fluid system starts to move at a certain moment of time. The generator velocity is assumed in the following form (Wilde and Wilde 2001)

$$v_g(t) = \frac{dx_g}{dt} = A_m\left\{1 - \left[1 + \tau + \frac{\tau^2}{2!} + \cdots + \frac{\tau^n}{n!}\right]\exp(-\tau)\right\}, \quad \tau = \eta t, \tag{48}$$

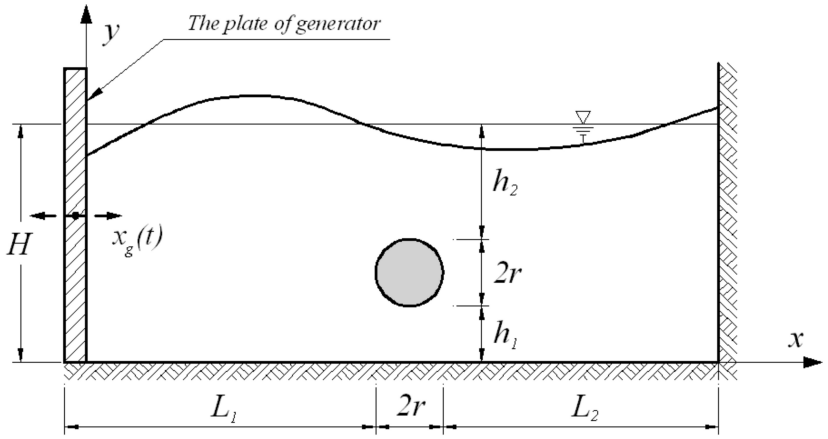

Fig. 4. Rectangular fluid domain with circular cylinder

where A_m is the velocity amplitude, η is a positive parameter responsible for a growth in time of the generator velocity, and τ is the dimensionless time.

One can check that at $t = 0$, the generator velocity, together with its acceleration and time derivatives up to the $n$order are all equal to zeros. With growing value of time the velocity (48) goes to the velocity amplitude (the expression within the brackets goes to unit value). With the assumed velocity, two cases of flow generation are considered. The first one, shown schematically in Fig. 5a, describes a half pulse of the generator plate and the second one, shown in Fig. 5b, denotes a finite pulse with zeros velocity and displacement at the end point of time.

In the numerical solution, the distribution of material particles in the problem domain together with their velocities and pressure distribution over the circular cylinder are calculated at chosen moments of time. The calculations have been performed for the non-viscous and viscous fluid as well. The discrete solution of the problem is reduced to integration in time of the continuity and momentum equations written for all the material particles. For each particle, we have the following system of differential equations

$$\frac{d\rho_a}{dt} = M_a, \quad \frac{d\boldsymbol{v}_a}{dt} = \boldsymbol{F}_a, \quad \frac{d\boldsymbol{x}_a}{dt} = \boldsymbol{G}_a, \tag{49}$$

where:

$$M_a = \sum_b m_b(\boldsymbol{v}_a - \boldsymbol{v}_b)\nabla_a W_{ab} \tag{50}$$

and

$$\boldsymbol{F}_a = -\sum_b m_b \left(\frac{p_a}{\rho_a^2} + \frac{p_b}{\rho_b^2}\right)\nabla_a W_{ab} + \boldsymbol{b}_a + \boldsymbol{T}_a. \tag{51}$$

In this equation $\boldsymbol{b}_a = (0, -g)$ denotes the gravity acceleration vector, and $\boldsymbol{T}_a$ describes the shear forces for the viscous fluid. The term $\boldsymbol{G}_a$ in the third equation in (49) denotes

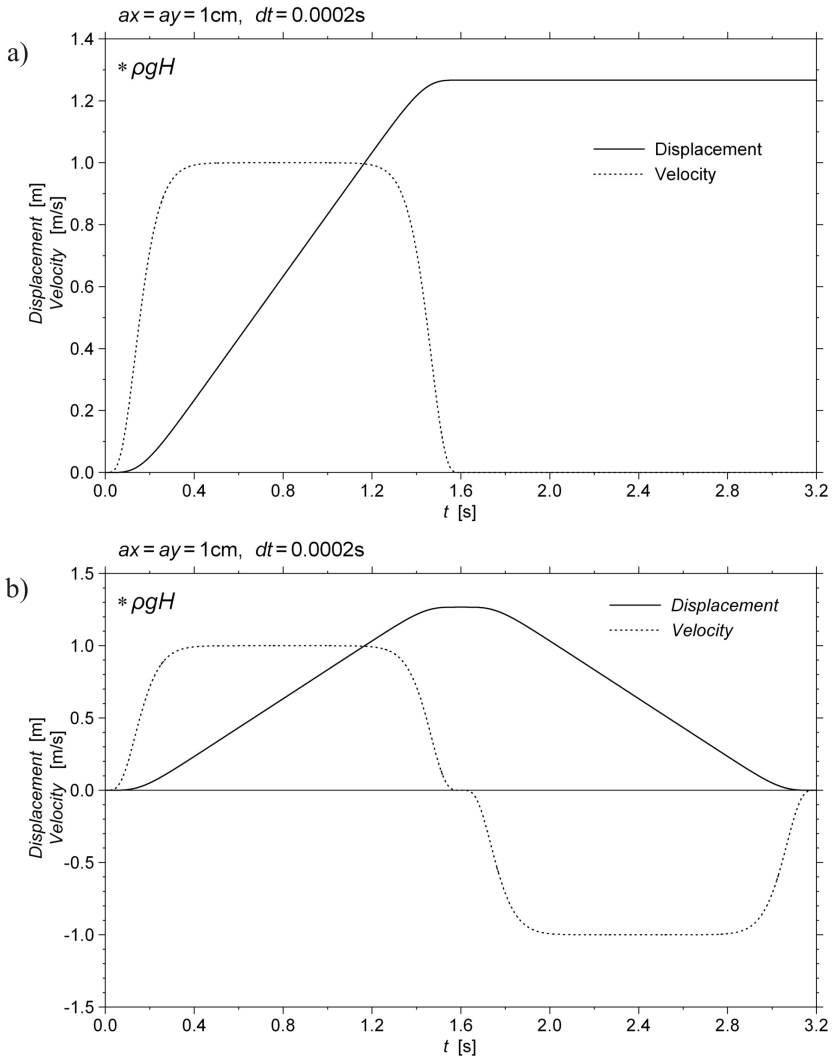

Fig. 5. Velocity and displacement of the generator plate

a corrected velocity of particle a. The velocity correction is assumed in the form as proposed by Monaghan (1992)

$$\boldsymbol{G}_a = \boldsymbol{v}_a + \sum_b \frac{m_a}{\rho_a + \rho_b}(\boldsymbol{v}_b - \boldsymbol{v}_a)W_{ab}, \tag{52}$$

which aims at smoothing velocity of a given particle.

For consistency, the corrected velocities are also used in equation (50). Similar correction is performed for the density field at chosen moments of time by means of

the formula

$$\rho_a = \sum_b m_b W_{ab}. \tag{53}$$

The evolution equations (49) are integrated numerically in the discrete time domain by applying an explicit two steps predictor – corrector scheme. Thus, in the first step, the mid-step value of the particle density, velocity and position are calculated

$$\rho_a^{k+1/2} = \rho_a^k + \frac{\Delta t}{2} M_a^k, \quad \boldsymbol{v}_a^{k+1/2} = \boldsymbol{v}_a^k + \frac{\Delta t}{2} F_a^k, \quad \boldsymbol{x}_a^{k+1/2} = \boldsymbol{x}_a^k + \frac{\Delta t}{2} \boldsymbol{G}_a^k, \tag{54}$$

where $\Delta t = t^{k+1} - t^k$ is the time step length.

Then, in the second, final step, the values of the dependent variables are calculated according to the formulae

$$\rho_a^{k+1} = \rho_a^k + \Delta t\ M_a^{k+1/2}, \quad \boldsymbol{v}_a^{k+1} = \boldsymbol{v}_a^k + \Delta t\ \boldsymbol{F}_a^{k+1/2}, \quad \boldsymbol{x}_a^{k+1} = \boldsymbol{x}_a^k + \Delta t\ \boldsymbol{G}_a^{k+1/2}. \tag{55}$$

In order to ensure the stability of the numerical integration, the time step Δt should satisfy the so called CFL condition that the speed of the initial particle spacing be greater than the reference speed (in our case the sound speed) (Toro 1997). With respect to a barotropic fluid with the bulk modulus κ and the sound speed $c = \sqrt{\gamma\kappa/\rho_0}$, the use of the real bulk modulus for water in the equation of state would result in extremely small time steps (Bonet and Lok 1999). Therefore, an artificial smaller bulk modulus has been used in such a way, that, instead of the sound speed, a certain maximum velocity given by equation (7) with $\rho_0 = 10^3$ Pa and $\rho_0 = 10^3$ kg/m^3 was taken into account. The evolution equations (49) were integrated with the time step of length $\Delta t = 2 \times 10^{-4}$ s. The initial conditions at $t = 0$ were those for the generator – fluid system at rest. Numerical solutions have been conducted for the non-viscous ($\boldsymbol{T}_a = \boldsymbol{0}$ in equation (51)), and viscous ($\boldsymbol{T}_a \neq \boldsymbol{0}$) fluids, as well. As it has been expected, the differences between solutions for the viscous and non-viscous fluids were so small (the differences were of second order small quantities) that in analysis of the aforementioned problem, the laminar viscosity of the fluid may be ignored. In fact, the spacing of the material particles was to big to describe changes within boundary layers of very mall thickness, where theinfluence of fluid viscosityon finial results may be significant.important. Some of the results obtained in computations are presented in the subsequent figures. The plots in figures 6 and 7 show the evolution in time of positions of the material particles and their dimensionless velocities, calculated according to the formula

$$\boldsymbol{v}_e = \frac{\boldsymbol{v}}{|\boldsymbol{v}_{\max}|}, \quad |\boldsymbol{v}_{\max}| = \sqrt{(u^2 + v^2)_{\max}}, \tag{56}$$

velocities for the generation presented in these plots correspond to the flow generation as presented in Fig. 5, respectively 5a. The next figure (8) shows the distribution of pressure over the cylinder for the flow generation presented in Fig. 5a. And finally,

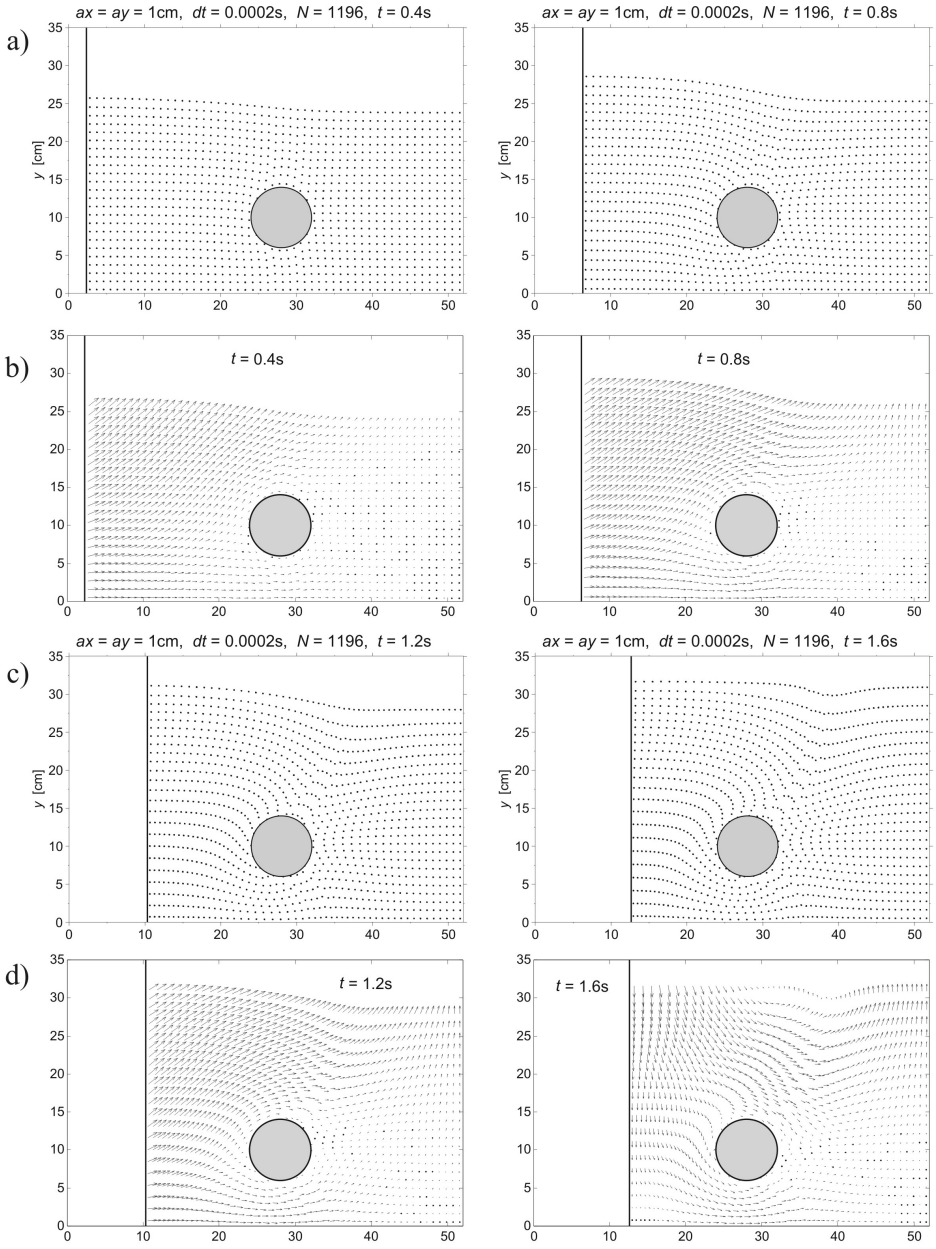

Fig. 6. The evolution in time of the material particles a), and their velocities b) for the generation presented in Fig. 5a

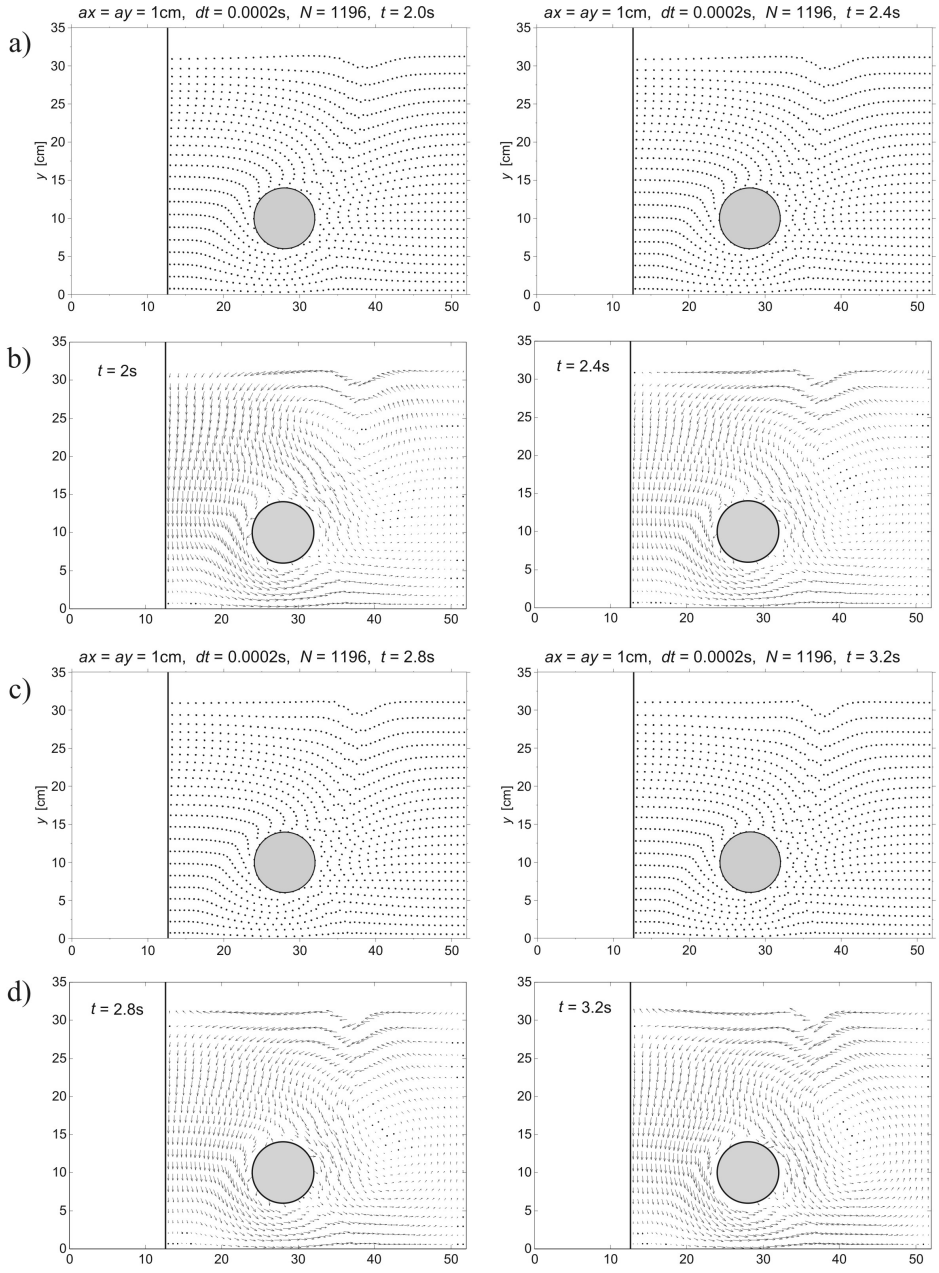

Fig. 7. The evolution in time of the material particles a), and their velocities b) for the generation presented in Fig. 5b

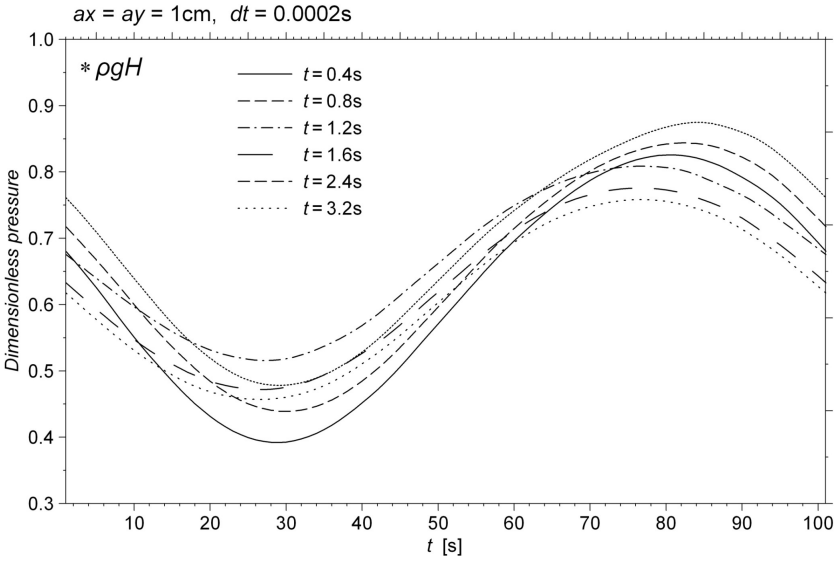

Fig. 8. The distribution of pressure over the cylinder for the generation presented in Fig. 5a

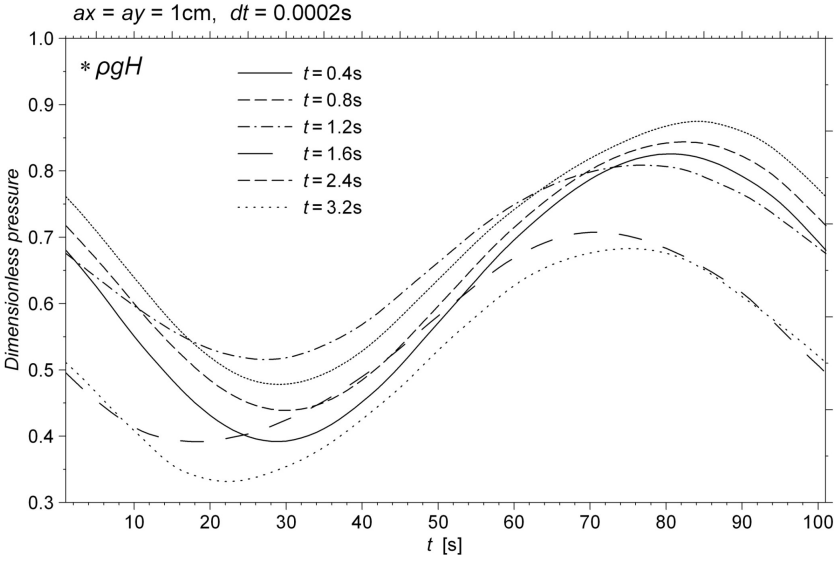

Fig. 9. The distribution of pressure over the cylinder for the generation presented in Fig. 5b

the plots in Fig. 9 illustrate the evolution of pressure for the flow generation as illustrated in Fig. 5b. From the plots it may be seen, that the SPH formulation seem to be sufficiently accurate to describe main features of behaviour of the fluid body, even for the case of big displacements of the fluid particles. It is difficult however to access the method accuracy, since it may be different in different areas of the fluid domain. For instance, it is reasonable to expect a lower accuracy in description of the flow

within areas close to the fluid boundaries. Nevertheless, the SPH formulation seems to be advantageous over mesh methods, especially in describing big displacements and possible discontinuities of fluid flows. The weak side of the method is that it needs a relatively large number of fluid particles to simulate a fluid flow and thus it needs a large time of computer work.

7. Concluding Remarks

The paper presents a discussion on boundary conditions and approximations in the description of shear forces for viscous fluids in the SPH description of water flows in the rectangular fluid domain with a circular cylinder in it. Close attention has been paid on boundary conditions at curved solid – fluid boundaries of the problem domain. In order to calculate the shear forces for viscous fluids, approximate description of interaction forces for a pair of particles was formulated in which differentiation of the stress components has been substituted by difference quotients of associated shear forces. Such a formulation reduces the order of the space differentiation of the velocity field by one. In this way, the solution to the viscous fluids is similar in nature to solution for non-viscous fluids. The numerical examples illustrate the ability of the SPH method to describe flows around a circular cylinder for the non-viscous and viscous fluids, as well. The SPH formulation is capable to describe the main features of the flow around the cylinder. It leads to accurate results in the fluid domain , except for the solid boundary areas where a certain deterioration of the numerical results may occur. It should be stressed that this solution to the boundary conditions at the fluid – cylinder interface is only a certain approximation, consistent with the discrete method employed.

References

Ataie-Ashtiani B., Shobeyri and Farhadi L. (2008) Modified incompressible SPH method for simulating free surface problems, *Fluid Dynamics Research*, **40**, 637–661.

Bonet J. and Lok T.-S. L. (1999) Variational and momentum preservation aspects of Smooth Particle Hydrodynamic formulations, *Comp. Methods in Appl. Mech. Engrg.*, **180**, 97–115.

Colagrossi A. and Landrini M. (2003) Numerical simulation of interfacial flows by smoothed particle hydrodynamics, *J. Comp. Phys.*, **191** (2), 448–475.

Dalrymple R. A. and Rogers B. D. (2006) Numerical modeling of water waves with the SPH Method, *Coastal Engineering*, **53**, 141–147.

Gomez-Gesteira M., Cerqueiro D., Crespo C. and Dalrymple R. A. (2005), Green water overtopping analysed with a SPH model, *Ocean Engineering*, **32**, 223–238.

Grenier N., Antuono M., Colagrossi A., Le Touze D. and Alessandrini B. (2009) An Hamiltonian interface SPH formulation for multi-fluid and free surface flows, *J. Computational Physics*, **228**, 8380–8393.

Hu X. Y. and Adams N. A. (2006) A multi-phase SPH method for macroscopic and mesoscopic flows, *J. Computational Physics*, **213**, 844–861.

Landau L. D. and Lifszyc J. M. (2009) *Hydrodynamika* (in Polish), PWN, Warszawa.

Liu G. R. and Liu M. B. (2009) *Smoothed Particle Hydrodynamics: A Mesh-free Particle Method*, World Scientific, Singapore.

Lo E. Y. M. and Shao S. (2002) Simulation of near-shore solitary wave mechanics by an incompressible SPH method, *Applied Ocean Research*, **24**, 275–286.

Monaghan J. J. and Gingold R. A. (1983) Shock Simulation by the Particle Method SPH, *J. of Computational Physics*, **52**, 374–389.

Monaghan J. J. (1992) Smoothed Particle Hydrodynamics, *Annual Rev. Astrophysics*, **30**, 543–574.

Monaghan J. J. (2005) Smoothed Particle Hydrodynamics, *Reports on Progress in Physics*, **68**, 1703–1759.

Monaghan J. J. and Kajtar J. B. (2009) SPH particle boundary forces for arbitrary boundaries, *Computer Physics Communications*, **180**, 1811–1820.

Monaghan J. J. (2012) Smoothed Particle Hydrodynamics and Its Diverse Applications, *Ann. Rev. Fluid Mech.*, **44**, 323–346.

Morris J. P., Fox P. J. and Zhu Y. (1997) Modeling Low Reynolds Number Incompressible Flows Using SPH, *J. Computational Physics*, **136**, 214–226.

Staroszczyk R. (2010) Simulation of Dam-Break Flow by a Corrected Smoothed Particle Hydrodynamics Method, *Archives of Hydro-Engineering and Environmental Mechanics*, **57** (1), 61–79.

Toro E. F. (1997) *Rieman Solvers and Numerical Methods for Fluid Dynamics*, Springer-Verlag, Berlin, Heidelberg.

Wilde P. and Wilde M. (2001) On the generation of water waves in a flume, *Archives of Hydro-Engineering and Environmental Mechanics*, **48** (4), 69–83.